Transverse spin dependent azimuthal correlations of charged pion pairs in $p^\uparrow p$ collisions at $\sqrt{s} = 510$ GeV at STAR

Navagyan Ghimire, for the STAR collaboration[a,*]

[a]*Department of Physics, Temple University,
1925 N. 12th St., Philadelphia, USA*

E-mail: navagyan.ghimire@temple.edu

The transverse polarization of quarks within a transversely polarized nucleon, $h_1^q(x)$, can only be accessed through processes involving its coupling with another chiral-odd functions, such as the spin-dependent interference fragmentation function (IFF) in polarized proton-proton collisions. The coupling of $h_1^q(x)$ and IFF leads to a measurable azimuthal correlation asymmetry ($A_{UT}^{\sin(\phi_{RS})}$) of di-hadron pairs in the final state. In previous work, the STAR experiment at RHIC measured a non-zero $A_{UT}^{\sin(\phi_{RS})}$ using polarized proton-proton ($p^\uparrow p$) data from 2011 at $\sqrt{s} = 500$ GeV, with an integrated luminosity of 25 pb^{-1}. The precise measurement of $A_{UT}^{\sin(\phi_{RS})}$ together with unpolarized di-hadron cross section will help to constrain the $h_1^q(x)$ in the global fits. In 2017, the STAR experiment collected dataset of approximately 350 pb^{-1} from $p^\uparrow p$ collisions at $\sqrt{s} = 510$ GeV. This new dataset will significantly improve the statistical precision of the $A_{UT}^{\sin(\phi_{RS})}$ measurement. In this proceedings, we will present preliminary result of the measurement of $A_{UT}^{\sin(\phi_{RS})}$ for pion pairs in the pseudorapidity region $|\eta| < 1$ based on the STAR 2017 $p^\uparrow p$ dataset.

---

*Speaker

1. Introduction

The internal structure of fast-moving hadrons comprises a large number of quarks and gluons collectively known as partons. The number densities of these partons in fast-moving hadrons are described by parton distribution functions (PDFs). In a collinear framework, integrating the transverse momentum of partons (k_T), at leading twist the spin structure of spin-$\frac{1}{2}$ hadrons (such as nucleons) can be characterized by three fundamental PDFs: unpolarized PDF ($f_1(x)$), helicity PDF ($g_1(x)$), and transversity PDF ($h_1^q(x)$).

Unlike $f_1(x)$ and $g_1(x)$, $h_1^q(x)$ is a chiral-odd distribution. It necessitates coupling with another chiral-odd distribution to appear in any observable and is consequently the least known fundamental PDF. $h_1^q(x)$ can be measured through single-hadron production in semi-inclusive deep-inelastic scattering (SIDIS) or in hadronic collisions. Alternatively, it can also be accessed via di-hadron production in hadronic collisions with leading-twist collinear factorization, where $h_1^q(x)$ couple with Interference Fragmentation Function (IFF), $H_1^{\sphericalangle}(z, M_h^2)$.

Due to the chiral-odd nature of $h_1^q(x)$, only a few channels exist from which $h_1^q(x)$ can be extracted. One of the easy and convenient channels is the IFF channel, where partons from transversely polarized protons collide with unpolarized partons from unpolarized protons to form an excited state parton. This parton further fragments and hadronizes into a di-haron pair in the final state via the IFF channel. The difference in the probability of a transversely polarized quark producing a hadron pair with opposite signs is described by $H_1^{\sphericalangle}(z, M_h^2)$. This probability is non-vanishing only in the presence of residual interactions in the final state. The existence of final state interactions during the fragmentation process allows for at least two competing production channels, interfering through a non-vanishing phase. Consequently, this type of fragmentation is termed Interference Fragmentation Function, and the corresponding channel is referred to as the IFF channel. The transverse polarization of the fragmenting quark influences the azimuthal distributions of the final state hadron pair, leading to experimentally observable di-hadron azimuthal correlation asymmetry ($A_{UT}^{\sin(\phi_{RS})}$) [1–3]. The measurement of $A_{UT}^{\sin(\phi_{RS})}$ provides a means to probe $h_1^q(x)$, which is involved in the cross-section convoluted with $H_1^{\sphericalangle}(z, M_h^2)$. It is essential to achieve an independent extraction of $H_1^{\sphericalangle}(z, M_h^2)$ through other experiments, such as e^+e^- Belle measurements.

$h_1^q(x)$ has its direct connection with the quark tensor charge [4].

$$\delta u = \int_0^1 \mathrm{d}x\, h_1^{u_v}(x; \mu), \qquad \delta d = \int_0^1 \mathrm{d}x\, h_1^{d_v}(x; \mu) \tag{1}$$

where, $h_1^{u_v}(x; \mu) \equiv h_1^q - h_1^{\bar{q}}$ are the valance distribution, and μ is the renormalization scale.

These quark tensor charges play a crucial role in calculating the nucleon electric dipole moment based on those of the quarks. Additionally, the isovector tensor charge $g_T (=\delta u - \delta d)$, derived from the up and down quark tensor charges, is essential for nuclear beta decay, serving as a vital input for beyond the Standard Model (BSM) calculations. Therefore, precise knowledge of δu, δd, and g_T, as well as compatibility between different techniques used for their determination, relies on the accurate measurement and universality of $h_1^q(x)$. Hence, a precise measurement of $A_{UT}^{\sin(\phi_{RS})}$ aids in constraining $h_1^q(x)$ and testing the universality of the mechanism generating azimuthal correlations across SIDIS, e^+e^-, lattice QCD, and pp collisions.

2. Experiment and Dataset

The measurement of $A_{UT}^{\sin(\phi_{RS})}$ through the IFF channel in pp collisions requires the transverse polarization of one of the proton beams. The Relativistic Heavy-Ion Collider (RHIC) at Brookhaven National Laboratory (BNL) stands as the sole facility globally capable of conducting this analysis because of its unique ability to collide protons both longitudinally and transversely polarized, up to a center-of-mass energy ($\sqrt{s}$) of 510 GeV. For the $A_{UT}^{\sin(\phi_{RS})}$ measurement, the identification of hadrons in the final state is crucial. Therefore, the Solenoidal Tracker At RHIC (STAR) experiment emerges as the optimal detector choice within the RHIC facility because of its particle identification (PID) capability. The STAR detector is capable of providing a uniform magnetic field of 0.5 T and features multiple sub-detectors working simultaneously. The data utilized in this analysis were recorded at the STAR experiment in 2017, with an integrated luminosity of 320 pb^{-1} from transversely polarized pp collisions at $\sqrt{s}$ = 510 GeV, with an average beam polarization of 55%. The Time Projection Chamber (TPC) is one of the major subsystems of the STAR detector, employed for tracking, momentum reconstruction, and particle identification. The TPC covers mid-pseudorapidity ($-1 \lesssim \eta \lesssim 1$) and provides full 2π azimuthal coverage in the $\eta - \phi$ space [5]. The Time-of-Flight (TOF) system has the same coverage as the TPC and is used for the PID in conjunction with the TPC by measuring the time of flight of particles [6]. The Barrel Electromagnetic Calorimeter (BEMC) is used to trigger events and shares the same coverage as the TPC and TOF [7]. The pion pair purity represents the probability that both particles in a pair are pions. The combination of the TPC and TOF is employed to achieve 83-92% purity of pion pairs in the final state. The bunches of each proton beam in the RHIC ring are transversely polarized up or down alternately with respect to the accelerator plane. However, when the $A_{UT}^{\sin(\phi_{RS})}$ is measured with respect to a given beam, the polarization of the other beam is integrated over to effectively be unpolarized. Elastic scattering of protons on ultra thin carbon ribbon tragets provides the relative polarization measurements on fill-by-fill basis, which is further calibrated to obtain the absolute polarization using the hydrogen gas jet polarimeter.

3. Analysis

The detection of two hadrons in the final state via the IFF channel allows us to relate the transverse polarization of the fragmenting quark to the transverse component of the difference of momentum vectors of the two hadrons in the final state. The relationship is defined using the mixed product in Eq. 2 and maintains the collinear framework [2, 3, 8, 9].

$$\vec{s_a} \cdot (\vec{R} \times \vec{p_h}) \qquad (2)$$

where, $\overrightarrow{p}_h = \vec{p}_{h,1} + \vec{p}_{h,2}$ and $\overrightarrow{R} = (\vec{p}_{h,1} - \vec{p}_{h,2})/2$ are the sum and difference of momentum vectors $\vec{p}_{h,1}$ and $\vec{p}_{h,2}$ of two hadrons in the final state repectively, and $\overrightarrow{s_a}$ contains the spin information of the fragmentating qurak.
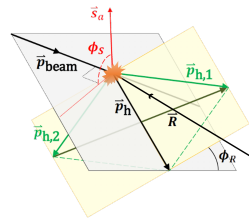
Figure 1: Azimuthal angle definitions in the di-hadron system. $\vec{p}_{h,1(2)}$ represents the momentum of the positive (negative) pion, while $\vec{s_a}$ indicates the beam polarization. ϕ_S is the angle between the beam polarization ($\vec{s_a}$) and the scattering plane (gray), and ϕ_R is the angle between the scattering plane and the di-hadron plane.

The cross-section of such process couples the $h_1^q(x)$ with $H_1^{\sphericalangle}(z, M_h^2)$ [10], which gives the probability of fragmenting the quark into hadron pairs in the final state, with sinusoidal modulation angle difference between scattering plane and di-hadron plane as illustrated in the Fig. 1.

$$d\sigma_{UT} \propto \sin(\phi_{RS}) \int dx_a dx_b f_1(x_b) h_1(x_a) \frac{d\Delta\hat{\sigma}}{d\hat{t}} H_{1,c}^{\sphericalangle}(z, M_h^2) \tag{3}$$

This sinusoidal modulation gives experimentally observable $A_{UT}^{\sin(\phi_{RS})}$.

$$A_{UT}^{\sin(\phi_{RS})} = \frac{d\sigma_{UT}}{d\sigma_{UU}} = \frac{d\sigma^\uparrow - d\sigma^\downarrow}{d\sigma^\uparrow + d\sigma^\downarrow} \propto \frac{h_1^q(x) H_1^{\sphericalangle}(z, M_h^2)}{f_1(x) D_1(z, M_h^2)} \tag{4}$$

The extraction of $h_1^q(x)$ from the $A_{UT}^{\sin(\phi_{RS})}$ measurement requires $H_1^{\sphericalangle}(z, M_h^2)$, unpolarized di-hadron fragmentation function ($D_1(z, M_h^2)$), and $f_1(x)$ provided by some other independent measurements. $f_1(x)$ is known precisely from DIS and SIDIS measurements. $e^+ e^-$ data from Belle experiment can provide valuable information about $H_1^{\sphericalangle}(z, M_h^2)$. The measurement of unpolarized di-hadron cross section in pp collision is essential to constrain the highly uncertain $D_1(z, M_h^2)$ specifically for gluon fragmentation in addtion to Belle $e^+ e^-$ measurement [11].

The azimuthal angles for measuring $A_{UT}^{\sin(\phi_{RS})}$ are defined according to the specifications outlined in Ref. [3], as illustrated in Fig. 1. The scattering plane is defined by the direction of the polarized proton beam ($\vec{p}_{beam}$), and the direction of the total momentum ($\vec{p}_h$) the pion pair. The di-pion plane is determined by the momentum vectors of each pion in the pair, $\vec{p}_{h,1}$ and $\vec{p}_{h,2}$. The difference vector ($\vec{R}$) resides in the di-hadron plane. The angle between the scattering plane and the polarization of the incident beam ($\vec{s}_a$) is termed ϕ_S. Additionally, the angle between the scattering plane and the di-hadron plane is denoted as ϕ_R. The angles ϕ_S and ϕ_R are calculated using Eq. 5 to 8 and are used to define the angle ϕ_{RS}, where $\phi_{RS} = \phi_R - \phi_S$. This angle modulates the polarized cross-section, and thus $A_{UT}^{\sin(\phi_{RS})}$ by $\sin(\phi_{RS})$, as detailed in Ref. [3, 12].

$$\cos(\phi_S) = \frac{\hat{p}_{beam} \times \vec{p}_h}{|\hat{p}_{beam} \times \vec{p}_h|} \cdot \frac{\hat{p}_{beam} \times \vec{s}_a}{|\hat{p}_{beam} \times \vec{s}_a|} \tag{5}$$

$$\sin(\phi_S) = \frac{(\vec{p}_h \times \vec{s}_a) \cdot \hat{p}_{beam}}{|(\hat{p}_{beam} \times \vec{p}_h)||\hat{p}_{beam} \times \vec{s}_a|} \tag{6}$$

$$\cos(\phi_R) = \frac{\hat{p}_h \times \vec{p}_{beam}}{|\hat{p}_h \times \vec{p}_{beam}|} \cdot \frac{\hat{p}_h \times \vec{R}}{|\hat{p}_h \times \vec{R}|} \tag{7}$$

$$\sin(\phi_R) = \frac{(\vec{p}_{beam} \times \vec{R}) \cdot \hat{p}_h}{|(\hat{p}_h \times \vec{p}_{beam})||\hat{p}_h \times \vec{R}|} \tag{8}$$

For azimuthally symmetric detectors such as STAR, the calculation of $A_{UT}^{\sin(\phi_{RS})}$ can be performed using the cross-ratio method outlined in Eq. 9. This method is inherently free from luminosity and efficiency dependencies in the determination of $A_{UT}^{\sin(\phi_{RS})}$ at the leading order, because of the combination of different polarization directions and symmetric detector hemispheres [13].

$$A_{UT}^{\sin(\phi_{RS})} \cdot \sin(\phi_{RS}) = \frac{1}{P} \cdot \frac{\sqrt{N^\uparrow(\phi_{RS}) N^\downarrow(\phi_{RS} + \pi)} - \sqrt{N^\downarrow(\phi_{RS}) N^\uparrow(\phi_{RS} + \pi)}}{\sqrt{N^\uparrow(\phi_{RS}) N^\downarrow(\phi_{RS} + \pi)} + \sqrt{N^\downarrow(\phi_{RS}) N^\uparrow(\phi_{RS} + \pi)}} \tag{9}$$

¹⁰⁵ where, P is the beam polarization and $N^{\uparrow(\downarrow)}$ is the number of pion pairs when the beam polarization
¹⁰⁶ is up (down).

¹⁰⁷   Two oppositely charged pions are paired if they exhibit proximity in $\eta - \phi$ space, satisfying
¹⁰⁸ $\sqrt{(\eta_{h,1} - \eta_{h,2})^2 + (\phi_{h,1} - \phi_{h,2})^2} \leq 0.7$, where $\eta_{h,1(2)}$ and $\phi_{h,1(2)}$ represent the pseudorapidity and
¹⁰⁹ azimuthal angle of the positive (negative) pion in the pair. The total momentum, $p_T^{\pi^+\pi^-}$, for each
¹¹⁰ pion pair must exceed 2.60 GeV/c. ϕ_{RS} is divided into 16 uniform bins spanning $[0, 2\pi]$, and
¹¹¹ the number of pion pairs in each ϕ_{RS} bin is counted to evaluate the right-hand side of Eq. 9.
¹¹² This result is then subjected to a fit using a single-parameter sinusoidal function over the interval
¹¹³ $[0, \pi]$ to extract $A_{UT}^{\sin(\phi_{RS})}$ as the amplitude of the fit. The $A_{UT}^{\sin(\phi_{RS})}$ is measured as a function of
¹¹⁴ pseudorapidity ($\eta^{\pi^+\pi^-}$), invarient mass ($M_{inv}^{\pi^+\pi^-}$), and $p_T^{\pi^+\pi^-}$ of pion pair.

¹¹⁵   The utilization of both TPC and TOF detectors simultaneously for PID results in a higher level
¹¹⁶ of pion purity compared to relying solely on TPC for PID. However, due to the lower efficiency of
¹¹⁷ TOF, not all events provide TOF information. Hence, the absolute difference between the $A_{UT}^{\sin(\phi_{RS})}$
¹¹⁸ calculated from samples with simultaneous TPC and TOF PID and those calculated from TPC PID
¹¹⁹ alone is employed as one of the systematic uncertainties (σ_{PID}). This refined PID leads σ_{PID} to be
¹²⁰ only a few percentage of the maximum $A_{UT}^{\sin(\phi_{RS})}$ signal.

¹²¹   The triggering mechanics in STAR contribute to the enhancement of quark-initiated jets [14].
¹²² To explore the potential bias effect introduced by the triggers, final state particles are generated in
¹²³ simulated pp events using PYTHIA 6.4.26 [15] with the Perugia-12 tune. For the better agreement
¹²⁴ of simulation and STAR data, slight modifications are made to the PARP(90) parameter in the
¹²⁵ Perugia-12 tune, as outlined in [16, 17]. Furthermore, these final state particles are passed through
¹²⁶ the STAR detector simulator GEANT 3 [18]. The ratio of the quark/parton ratio from the biased
¹²⁷ sample (detector level) to the quark/parton ratio from the unbiased sample (PYTHIA level) is
¹²⁸ utilized to compute the systematic uncertainty associated with trigger bias (σ_{trig}). σ_{trig} is found
¹²⁹ to be 2 - 20% of $A_{UT}^{\sin(\phi_{RS})}$ signal, depending on the kinematic variables. The total systematic
¹³⁰ uncertainty is defined as $\sigma_{\mathrm{tot}} = \sqrt{\sigma_{\mathrm{PID}}^2 + \sigma_{\mathrm{trig}}^2}$.

4. Results

¹³²   Since the quantity $A_{UT}^{\sin(\phi_{RS})}$ arises from the convolution of $h_1^q(x)$ and $H_1^{\sphericalangle}(z, M_h^2)$ modulated by
¹³³ $sin(\phi_{RS})$, $A_{UT}^{\sin(\phi_{RS})}$ is measured as a function of $\eta^{\pi^+\pi^-}$, which is intricately linked to the partonic
¹³⁴ variable x through $h_1^q(x)$. $A_{UT}^{\sin(\phi_{RS})}$ is also measured with respect to $p_T^{\pi^+\pi^-}$ and $M_{inv}^{\pi^+\pi^-}$ which, in
¹³⁵ turn, is associated with $H_1^{\sphericalangle}(z, M_h^2)$ through final state variable z, fractional energy carried by the
¹³⁶ hadron pair from the fragmentating quark, and invarient mass of pion pair in the final state.

¹³⁷   A monotonic rise in the measured $A_{UT}^{\sin(\phi_{RS})}$ signal is observed with increasing $\eta^{\pi^+\pi^-}$, as
¹³⁸ depicted in Fig. 2. The direction of $\eta^{\pi^+\pi^-}$ is defined as forward (> 0) and backward (< 0),
¹³⁹ based on the direction of the momentum of the polarized beam. When $\eta^{\pi^+\pi^-} > 0$, it signifies the
¹⁴⁰ forward-propagating transversely polarized parton carrying a larger x value, typically in the valence
¹⁴¹ region. This leads to a sizable $h_1^q(x)$ and, consequently, a larger $A_{UT}^{\sin(\phi_{RS})}$ signal. Conversely, when
¹⁴² $\eta^{\pi^+\pi^-} < 0$, it indicates the backward-propagating transversely polarized parton carrying a lower x,
¹⁴³ resulting in a smaller transversity and a significantly suppressed $A_{UT}^{\sin(\phi_{RS})}$ signal.
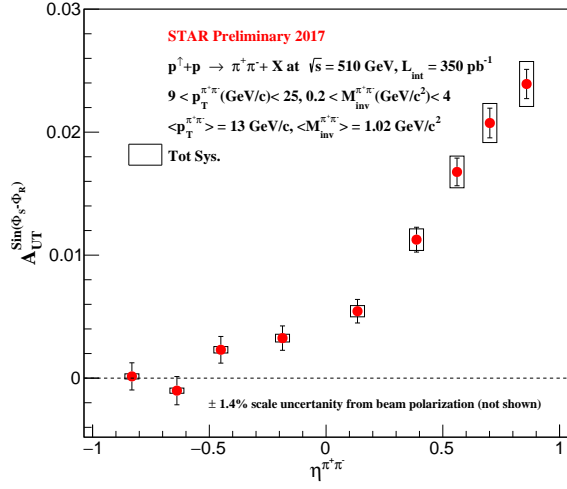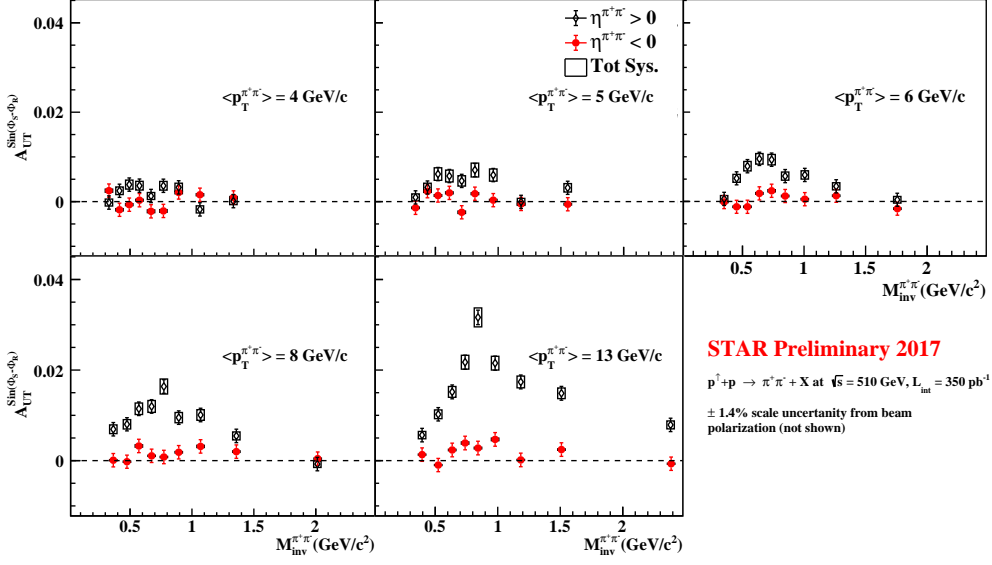
Figure 2: $A_{UT}^{\sin(\phi_{RS})}$ vs $\eta^{\pi^+\pi^-}$ for $\langle p_T^{\pi^+\pi^-} \rangle = 13$ GeV/c. The vertical lines represent statistical uncertainties, and open rectangular boxs represent systematic uncertainties.

The variation of $A_{UT}^{\sin(\phi_{RS})}$ with respect to $p_T^{\pi^+\pi^-}$ is illustrated in Fig. 3 for both $\eta^{\pi^+\pi^-} > 0$ (depicted in black) and $\eta^{\pi^+\pi^-} < 0$ (depicted in red), considering five distinct $M_{inv}^{\pi^+\pi^-}$ bins. A monotonically increasing $A_{UT}^{\sin(\phi_{RS})}$ signal is discernible as $p_T^{\pi^+\pi^-}$ increases in the forward direction, while a relatively smaller $A_{UT}^{\sin(\phi_{RS})}$ signal is observed in the backward direction as already seen in Fig. 2. Notably, a more pronounced rise in the signal is evident around the mass of the ρ meson, a phenomenon that will be further discussed below.
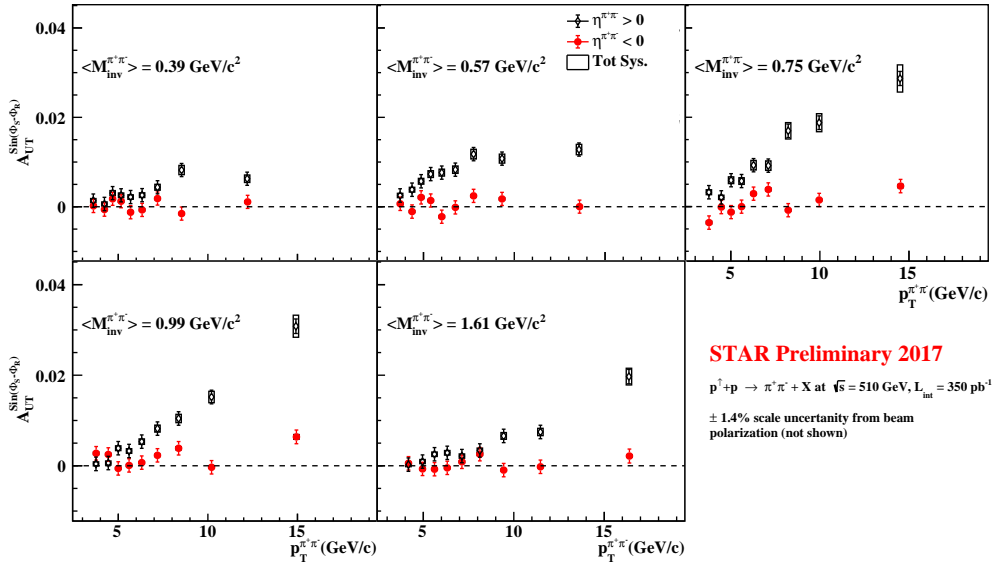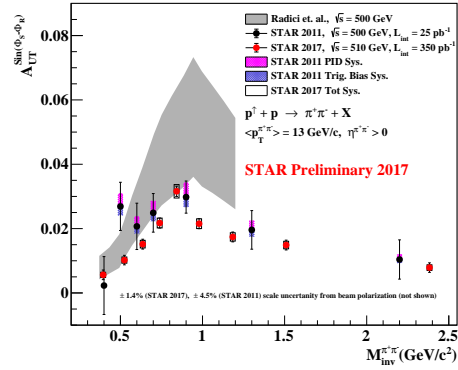

Figure 3: $A_{UT}^{\sin(\phi_{RS})}$ vs $p_T^{\pi^+\pi^-}$ for five $M_{inv}^{\pi^+\pi^-}$ bins. The black points represent $A_{UT}^{\sin(\phi_{RS})}$ for $\eta^{\pi^+\pi^-} > 0$, while red points correspond to $\eta^{\pi^+\pi^-} < 0$. The vertical lines indicate statistical uncertainties, and the open rectangular boxs represent systematic uncertainties.

Figure 4: $A_{UT}^{\sin(\phi_{RS})}$ vs $M_{inv}^{\pi^+\pi^-}$ for five $p_T^{\pi^+\pi^-}$ bins. The black points represent $A_{UT}^{\sin(\phi_{RS})}$ for $\eta^{\pi^+\pi^-} > 0$, while red points correspond to $\eta^{\pi^+\pi^-} < 0$. The vertical lines indicate statistical uncertainties, and the open rectangular boxes represent systematic uncertainties.

Figure 4 illustrates $A_{UT}^{\sin(\phi_{RS})}$ as a function of $M_{inv}^{\pi^+\pi^-}$ for both $\eta^{\pi^+\pi^-} > 0$ (depicted in black) and $\eta^{\pi^+\pi^-} < 0$ (depicted in red) across five distinct $p_T^{\pi^+\pi^-}$ bins. The plot exhibits the characteristic profile of the invariant mass dependence of the $H_1^\triangleleft(z, M_h^2)$, featuring a noticeable peak around the mass of the ρ resonance for di-pion pairs especially for $\eta^{\pi^+\pi^-} > 0$ for higher $p_T^{\pi^+\pi^-}$ bins. Model calculations, as documented in Ref. [2, 3, 9], elucidate that the transverse spin-dependent fragmentation function arises from the interference of amplitudes possessing different angular momenta. In the scenario of di-pion pairs, vector mesons decaying in a relative p-wave interfere with a non-resonant background in a relative s-wave, resulting in an observable enhancement of the $A_{UT}^{\sin(\phi_{RS})}$ signal around the mass of the ρ meson.

Figure 5: Comparison of $A_{UT}^{\sin(\phi_{RS})}$ vs $M_{inv}^{\pi^+\pi^-}$ for the highest $p_T^{\pi^+\pi^-}$ and $\eta^{\pi^+\pi^-} > 0$. The red points represent this analysis and black points represent STAR's previous result from 2011 data. The gray solid band represents the theoretical prediction by Radici et al. [19] utilizing existing SIDIS and e^+e^- data exclusively.

A comparison between the $A_{UT}^{\sin(\phi_{RS})}$ as functions of $M_{inv}^{\pi^+\pi^-}$ for $\eta^{\pi^+\pi^-} > 0$ in the highest $p_T^{\pi^+\pi^-}$ bin is depicted in Fig. 5, incorporating data from both the current analysis (red) and the published STAR 500 GeV result (black) [12]. Concurrently, theoretical prediction from Ref. [19]

are presented, where the theoretical prediction is based on $h_1^q(x)$ derived from SIDIS and $H_1^\sphericalangle(z, M_h^2)$ derived from the e^+e^- Belle measurement. The global extraction of transversity, leveraging the STAR 200 GeV and 500 GeV results, assumes a pivotal role in refining and constraining these theoretical predictions, as exemplified by the JAM collaboration [20].

The consistency of this new findings with the preceding STAR 2011 results is notable, accompanied by a marked improvement in precision at both statistical and systematic levels. The larger dataset, featuring an integrated luminosity of $L_{\text{int}} = 320$ pb^{-1}, nearly 13 times larger than the antecedent STAR 2011 dataset ($L_{\text{int}} = 25$ pb^{-1}), yields a fourfold enhancement in statistical precision. Moreover, the incorporation of TPC together with TOF detector for the PID serves as a crucial strategy in mitigating systematic uncertainties.

5. Summary and Outlook

This analysis measures the $A_{UT}^{\sin(\phi_{RS})}$ as functions of $\eta^{\pi^+\pi^-}$, $M_{inv}^{\pi^+\pi^-}$, and $p_T^{\pi^+\pi^-}$ to probe its sensitivity to $h_1^q(x)$ and $H_1^\sphericalangle(z, M_h^2)$ employing the STAR 2017 pp dataset. Notably, a discernible increase in $A_{UT}^{\sin(\phi_{RS})}$ is observed in the forward direction ($\eta^{\pi^+\pi^-} > 0$), attributed to the higher x values, where the quark transversity is anticipated to be substantial. Conversely, a lower $A_{UT}^{\sin(\phi_{RS})}$ signal corresponds to backward-propagating transversely polarized partons carrying lower x. The observed enhancement in the $A_{UT}^{\sin(\phi_{RS})}$ signal around the ρ meson aligns with model calculations. Furthermore, the $A_{UT}^{\sin(\phi_{RS})}$ exhibits a monotonic increase with $p_T^{\pi^+\pi^-}$. The utilization of a larger dataset coupled with a robust PID methodology facilitates precise $A_{UT}^{\sin(\phi_{RS})}$ measurements, enhancing the constraining power for global analyses.
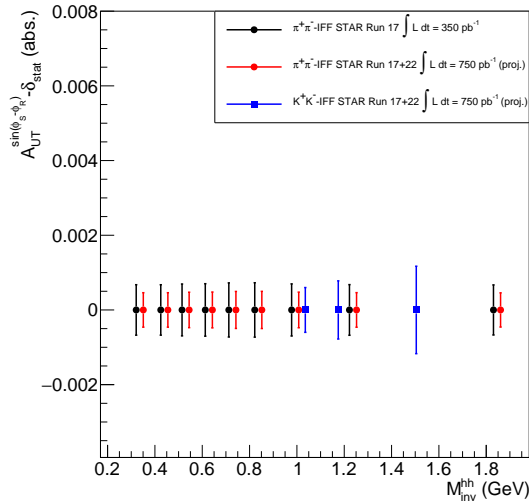
Figure 6: Statistical error projections of $\pi^+\pi^-$ (red) and K^+K^- (blue) $A_{UT}^{\sin(\phi_{RS})}$ measurements for STAR 2022 dataset. Black points represents the statistical uncertainties of $A_{UT}^{\sin(\phi_{RS})}$ from preliminary result of STAR 2017 dataset. Points are jittered horizontally for visual clearity.

STAR recently acquired a substantially larger pp dataset, amounting to $L_{\text{int}} = 400$ pb^{-1}, at a center-of-mass energy of $\sqrt{s} = 508$ GeV in 2022. This newly obtained dataset, in conjunction

with the previous STAR 2017 pp dataset, holds the potential to enhance the precision of di-pion asymmetry measurements as shown in Fig. 6. Furthermore, it enables the advancement of analysis through the incorporation of a 3D binning scheme in $\eta^{\pi^+\pi^-}$, $M_{inv}^{\pi^+\pi^-}$, and $p_T^{\pi^+\pi^-}$. This approach provides additional insights into the characteristics of $h_1^q(x)$ across these kinematic variables simultaneously.

The exploration of the flavor dependence of $h_1^q(x)$ becomes feasible by measuring asymmetry for various hadron pairs, such as K^+K^-, $K^+\pi^-(K^-\pi^+)$, and $\pi^+\pi^-$, in pp collisions. The combined dataset from 2017 and 2022 can be effectively utilized to measure di-hadron asymmetry for low multiplicity hadron pairs like K^+K^-, offering a unique avenue to probe s-quark transversity.

In addition to the $H_1^{\sphericalangle}(z, M_h^2)$, another crucial factor for constraining $h_1^q(x)$ is the $D_1(z, M_h^2)$. STAR is planning for measurements of unpolarized cross-section at $\sqrt{s} = 200$ and 500 GeV. These measurements aim to tighten the currently loosely constrained $D_1(z, M_h^2)$, particularly for the gluon fragmentation function, which lacks constraints from e^+e^- data.

References

[1] J. Tang, *Probing the nucleon's transversity via two meson production in polarized nucleon-nucleon collisions*, hep-ph/9807560.

[2] A. Bianconi, S. Boffi, R. Jakob and M. Radici, *Two hadron interference fragmentation functions. Part 1. General framework*, *Phys. Rev. D* **62** (2000) 034008 [hep-ph/9907475].

[3] A. Bacchetta and M. Radici, *Dihadron interference fragmentation functions in proton-proton collisions*, *Phys. Rev. D* **70** (2004) 094032 [hep-ph/0409174].

[4] JAM collaboration, *Transversity distributions and tensor charges of the nucleon: extraction from dihadron production and their universal nature*, 2306.12998.

[5] STAR collaboration, *STAR detector overview*, *Nucl. Instrum. Meth. A* **499** (2003) 624.

[6] M. Shao, O.Y. Barannikova, X. Dong, Y. Fisyak, L. Ruan, P. Sorensen et al., *Extensive particle identification with TPC and TOF at the STAR experiment*, *Nucl. Instrum. Meth. A* **558** (2006) 419 [nucl-ex/0505026].

[7] STAR collaboration, *The STAR barrel electromagnetic calorimeter*, *Nucl. Instrum. Meth. A* **499** (2003) 725.

[8] J.C. Collins and G.A. Ladinsky, *On pi - pi correlations in polarized quark fragmentation using the linear sigma model*, hep-ph/9411444.

[9] R.L. Jaffe, X.-m. Jin and J. Tang, *Interference fragmentation functions and the nucleon's transversity*, *Phys. Rev. Lett.* **80** (1998) 1166 [hep-ph/9709322].

[10] STAR collaboration, *Observation of Transverse Spin-Dependent Azimuthal Correlations of Charged Pion Pairs in $p^\uparrow + p$ at $\sqrt{s} = 200\ GeV$*, *Phys. Rev. Lett.* **115** (2015) 242501 [1504.00415].

[11] BELLE collaboration, *Observation of transverse polarization asymmetries of charged pion pairs in e^+e^- annihilation near $\sqrt{s}$ = 10.58 GeV*, *Phys. Rev. Lett.* **107** (2011) 072004 [1104.2425].

[12] STAR collaboration, *Transverse spin-dependent azimuthal correlations of charged pion pairs measured in $p^\uparrow$+p collisions at $\sqrt{s}$ = 500 GeV*, *Phys. Lett. B* **780** (2018) 332 [1710.10215].

[13] G.G. Ohlsen and P.W. Keaton, *Techniques for measurement of spin-1/2 and spin-1 polarization analyzing tensors*, *Nucl. Instrum. Meth.* **109** (1973) 41.

[14] STAR collaboration, *Longitudinal and transverse spin asymmetries for inclusive jet production at mid-rapidity in polarized p + p collisions at $\sqrt{s}$ = 200 GeV*, *Phys. Rev. D* **86** (2012) 032006 [1205.2735].

[15] T. Sjostrand, S. Mrenna and P.Z. Skands, *PYTHIA 6.4 Physics and Manual*, *JHEP* **05** (2006) 026 [hep-ph/0603175].

[16] STAR collaboration, *Underlying event measurements in p + p collisions at $\sqrt{s}$ = 200 GeV at RHIC*, *Phys. Rev. D* **101** (2020) 052004 [1912.08187].

[17] STAR collaboration, *Longitudinal double-spin asymmetry for inclusive jet and dijet production in pp collisions at $\sqrt{s}$ = 510 GeV*, *Phys. Rev. D* **100** (2019) 052005 [1906.02740].

[18] R. Brun, R. Hagelberg, M. Hansroul and J.C. Lassalle, *Simulation program for particle physics experiments, GEANT: user guide and reference manual*, CERN, Geneva (1978).

[19] M. Radici, A.M. Ricci, A. Bacchetta and A. Mukherjee, *Exploring universality of transversity in proton-proton collisions*, *Phys. Rev. D* **94** (2016) 034012 [1604.06585].

[20] C. Cocuzza, A. Metz, D. Pitonyak, A. Prokudin, N. Sato and R. Seidl, *First Simultaneous Global QCD Analysis of Dihadron Fragmentation Functions and Transversity Parton Distribution Functions*, 2308.14857.